Degradation of perfluorooctanoic acid using zero-valent iron coated by carboxymethyl-β-cyclodextrin polymer

Silvestri Daniele[a], Roberto Montarolo[b], Mohammad Gheibi[a], Dariusz Łukowiec[c], Michal Řezanka[a], Vinod V.T. Padil[d], Barbara Onida[b], Rajandrea Sethi[e], Miroslav Černík[a*], Mietek Jaroniec[f], and Stanisław Wacławek[a*]

[a]Institute for Nanomaterials, Advanced Technologies and Innovation, Technical University of Liberec, Studentská 1402/2, 461 17, Liberec 1, Czech Republic

[b]Department of Applied Science and Technology (DISAT), Politecnico di Torino, C.so Duca degli Abruzzi 24, 10129 Torino, Italy

[c]Materials Research Laboratory, Faculty of Mechanical Engineering, Silesian University of Technology, Konarskiego 18A St., 44–100 Gliwice, Poland

[d]Amrita School for Sustainable Futures Amrita Vishwa Vidyapeetham Amritapuri Campus Amritapuri, Clappana P. O. Kollam - 690525 Kerala, India

[e]Department of Environmental, Land and Infrastructure Engineering (DIATI), Politecnico di Torino, Corso Duca degli Abruzzi, 24, 10129 Turin, Italy

[f]Department of Chemistry and Biochemistry & Advanced Materials and Liquid Crystal Institute, Kent State University, Kent, OH 44242, USA

[*]Corresponding author: miroslav.cernik@tul.cz; jaroniec@kent.edu; stanislaw.waclawek@tul.cz

Contents

Experimental Section

Chemicals

Iron(III) chloride hexahydrate ($FeCl_3 \bullet 6H_2O$, purity ≥98%), sodium borohydride ($NaBH_4$, ≥98%), perfluorooctanoic acid ($C_8HF_{15}O_2$, 95%), sodium hydroxide (NaOH, ≥97%), hydrochloric acid (HCl, 37%) and methanol (≥99.9%) were purchased from Sigma-Aldrich, Czech Republic; soluble carboxymethyl-β-cyclodextrin polymer (≥95%) was purchased from CycloLab Ltd., Hungary; ethanol (96%) was purchased from PENTA s.r.o., Czech Republic. In all experiments, deionized water (DI) from ELGA LabWater was used (Veolia Water Solutions & Technologies), UK.

Analytical procedures

The spectra for mass spectrometry were recorded by LC–QTOF with MS detection using an Exion AC LC chromatograph and X500R QTOF mass spectrometric detector (LC-MS) (detection limit: PFHpA and PFHxA 12.5 µg/L, PFOA 7 µg/L, limit of quantitation: PFHpA and PFHxA 37.5 µg/L, PFOA 21 µg/L). The column used is Synergi Fusion-RP with 4 µm particle size and 50 mm length x 2 mm I. D. The mobile phase consists of 20 mM NH_4CO_2 in 5% Methanol as component A and Methanol as component B. The flow rate used is 0.4 ml/min and the temperature of the column is kept at 40°C. The gradient used for the determination is described in Tab. S1. Negative mode ESI ionization was used. The temperature of the ion source used was 500°C. The Gas 1 was set to 50 PSI, Gas 2 to 40 PSI and curtain gas was set to 35°C. To improve the reliability of the determination $^{13}C_8$PFOA and $^{13}C_8$PFOS were used as internal standards. The used transitions for analytes and the internal standards are displayed in Tab. S2. Acetate and formate were determined on ion chromatograph Thermo Scientific™ Dionex™ ICS-2100 with Regent-Free™ IC (RFIC™) system, equipped with conductivity detector and IonPac™ AS11-HC column (detection limit: 0.05 mg/L for both acetate and formate).

Characterization techniques

High-resolution transmission electron microscopy (HR-TEM) analysis was performed using a transmission electron microscopy/scanning transmission electron microscopy (TEM/STEM) (Titan 80-300, FEI, Eindhoven, The Netherlands) with a super twin-lens operated at 300 kV and equipped with an annular dark field detector. The presence of various elements was analyzed using energy-dispersive X-ray spectroscopy (EDX, Aztec, Oxford Instruments, Abingdon, UK). Zetasizer Nano ZS device (Malvern PANalytical Ltd, United Kingdom) with an autocorrelation function of 10 seconds was used to measure zeta potential (ζ-potential) of dispersed nanoparticles in DI water in triplicates. X-ray photoelectron spectroscopy (XPS) was carried out using a Physical Electronics VersaProbe instrument (Physical Electronics, Lake Drive, MN, USA), using Al radiation.

Synthesis of Fe-CMCD

One-step synthesis of nanoparticles was done based on a modified approach by Silvestri et al.[1] Firstly, both $FeCl_3 \bullet 6H_2O$ (0.2 M) and carboxymethyl-β-cyclodextrin (CMBCD) (16 g/L) were dissolved separately in DI water and stirred. After dissolution, both solutions were added (50 mL of $FeCl_3 \bullet 6H_2O$ and 25 mL of

CMBCD were added to 15 mL of DI) and mixed together at 200 RPM (mechanical stirring, HS-50A, WITEQ, Germany) for 15 min under N_2 atmosphere. Then, using a peristaltic pump (BT300LC, CRpump, China) $NaBH_4$ solution (5 M, 10 mL) was delivered at a flow rate of 5 mL/min. After titration of the reductant, the reaction mixture was left for an additional 10 min of stirring. The final concentration in the reaction mixture was 0.1 M of $FeCl_3 \bullet 6H_2O$, 0.5 M of $NaBH_4$ and 4 g/L of CMBCD. Synthesized iron-carboxymethyl-β-cyclodextrin (Fe-CMBCD) were separated by a strong magnet (MAGSY s.r.o., Czech Republic), washed 5 times with ethanol to remove residual impurities, and freeze-dried for 24 hours to obtain dried powder. Pristine nZVI was synthesized using the above-mentioned method, except no CMBCD was added.

Degradation tests

A defined volume of PFOA stock solution (1 g/L, the stock solution was prepared by heating it to 50 °C overnight) was dosed to deionized (DI) water to achieve the target final concentrations of PFOA (0.2, 2, or 500 mg/L) and transferred to an amber glass bottle. The suspension of nanoparticles was prepared by adding dried nFe-CMBCD powder to DI water, followed by homogenization using a dispenser (T25 digital ULTRA-TURRAX, IKA, Germany) at 12,000 RPM for one minute. From this suspension, an exact volume of nFe-CMBCD was introduced into the reaction glass of 20 or 50 mL to reach a final concentration of 5 g/L. The reaction mixture was continuously mixed using a laboratory rotator (RM-2L Intelli-mixer, ELMI, USA, 95 RPM) at 95 RPM. Samples for analysis were collected at specific time intervals, separated using a magnet, and filtered with syringe filters (CHS Filterpure PTFE, <0.22 μm). The initial pH levels (3, 5, 7, 9, and 11) were adjusted using either NaOH or HCl (0.1 M) and measured by SevenCompact pH meter S220 (Mettler Toledo).

Oxic and anoxic conditions

The samples were bubbled with N_2 (to establish an anoxic condition) or dried in air (to create an oxic condition) for 30 minutes. After bubbling, nFe-CMBCD was added to the reactor to initiate the degradation reaction. The reactors were kept under constant agitation throughout the entire duration of the test (RM-2L Intelli-mixer, ELMI, USA, 95 RPM). PFOA 500 mg/L, nFe-CMBCD 5 g/L.

Desorption tests

Desorption tests were carried out immediately after the absorption tests to minimize the material's contact time with the atmosphere. The solution was taken away and substituted with an equal amount of methanol (20 mL, ≥99.9%). Then, the reactor was kept under constant agitation for three days (RM-2L Intelli-mixer, ELMI, USA, 95 RPM). Afterward, an aliquot was taken and analyzed using LC-MS.

Characterization

Transmission electron microscope (TEM) analysis was conducted to evaluate the morphology of the nFe-CMBCD nanoparticles. The nanoparticles exhibit a spherical shape which is typical for nFe;[1] moreover, TEM analysis indicated the presence of a surface coating[2] by CMBCD (**Figure S1A**). Selected

area electron diffraction (SAED) patterns (inset **Figure S1A**) revealed the polycrystalline structure of the material.[3] The Energy dispersive X-ray (EDX) analysis showed the presence of Fe, O, and C attributable respectively to the presence of iron oxide and the polymer coating[4] (**Figure S1B**). The EDX profile (**Figure S1C-F**) reveals iron oxides on the surfaces of the nanoparticles. In addition, the uniform carbon distribution indicates the presence of the CMBCD polymer, confirming the successful synthesis of nFe-CMBCD.

X-ray photoelectron spectroscopy (XPS) analysis was performed to further elucidate the chemical state and elemental composition of nFe-CMBCD. **Figure S1G** shows a survey scan that reveals characteristic signals ascribed to iron, oxygen, and carbon.[5] Initially, the signal at ~284 eV (C 1s) was deconvoluted into three main peaks (**Figure S1H**). The peak at ~284.7 is ascribed to C—C,[5,6] while the signal at ~286.1 is compatible with the presence of C—O [2,6], the last peak (~288 eV) is assigned to O—C—O.[5,6] Similarly, the peak assigned to Fe $2p_{3/2}$ (~710 eV) was deconvoluted into five components (**Figure S1I**), identifying signals corresponding to Fe^{2+}, Fe^{3+} (in both octahedral[2] and tetrahedral coordination[7] at 709 and 711 eV, respectively), and Fe^{0} (at 706 eV) confirming the presence of mixed-valence iron species. The XPS results are in good agreement with the literature. In addition, these XPS results are consistent with the findings from EDX and further validate the inorganic-organic nature of nFe-CMBCD.

Figures

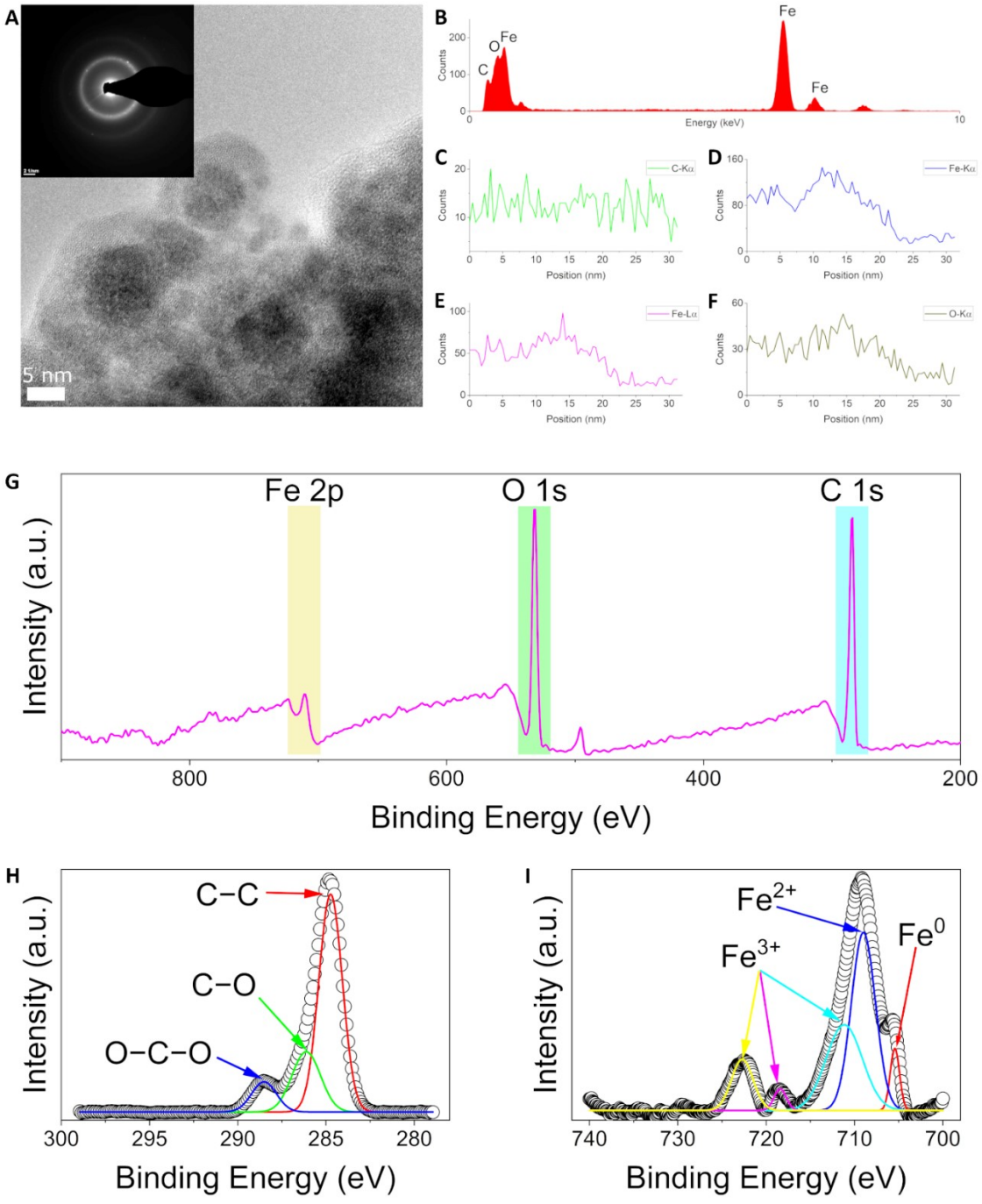

Figure S1 A) TEM analysis of nFe-CMBCD and SAED analysis (inset). B) EDX elemental profile. EDX Linescan Profiles of C) carbon Kα, d) Iron Kα, E) Iron Lα, and F) oxygen Kα. G) XPS survey scan of nFe-CMBCD, high-resolution narrow scans of H) C 1s and I) Fe $2p_{3/2}$.

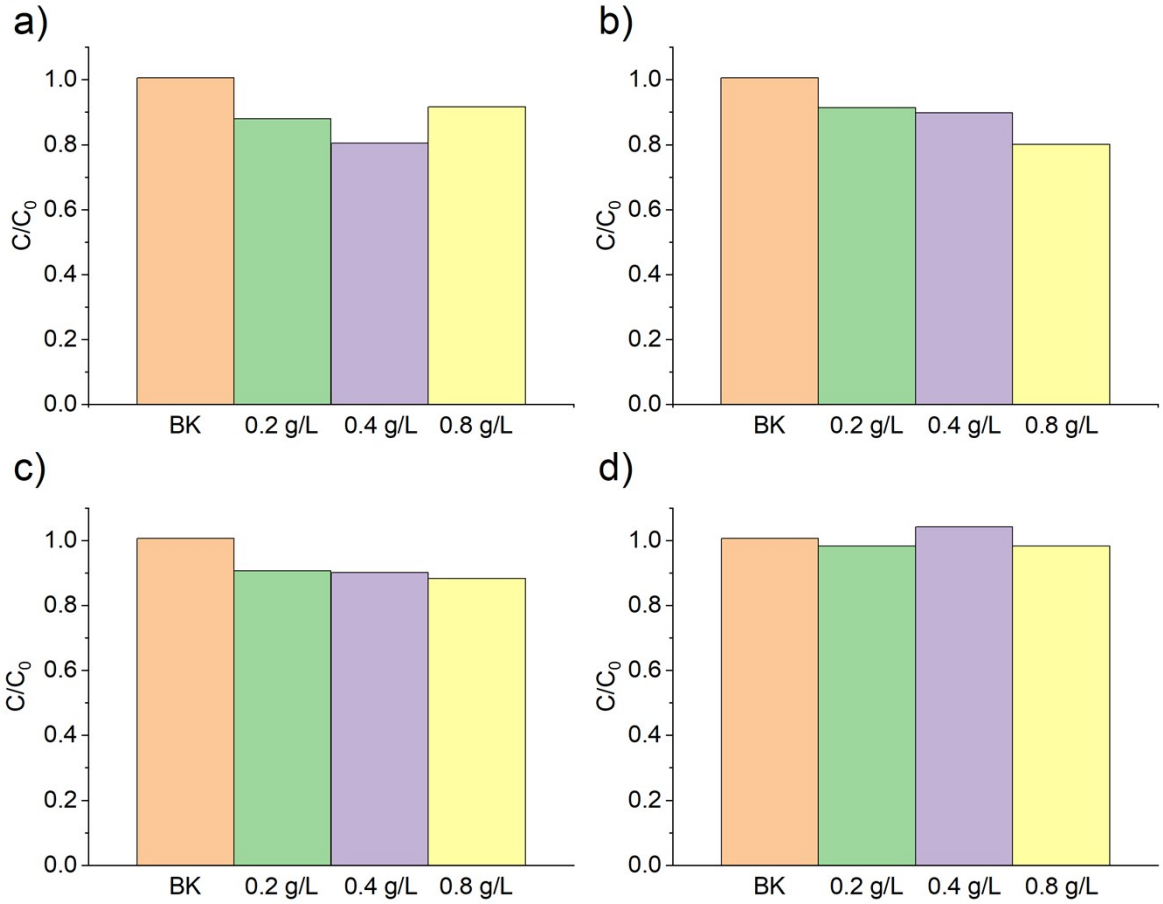

Figure S2 PFOA removal test using various CMBCD concentrations (0.2, 0.4, 0.8 g/L) at a) pH 5 (PFOA 0.2 mg/L), b) pH 5 (PFOA 2 mg/L), c) pH 7 (PFOA 0.2 mg/L) and d) pH 7 (PFOA 2 mg/L) (Blank= BK without CMBCD).

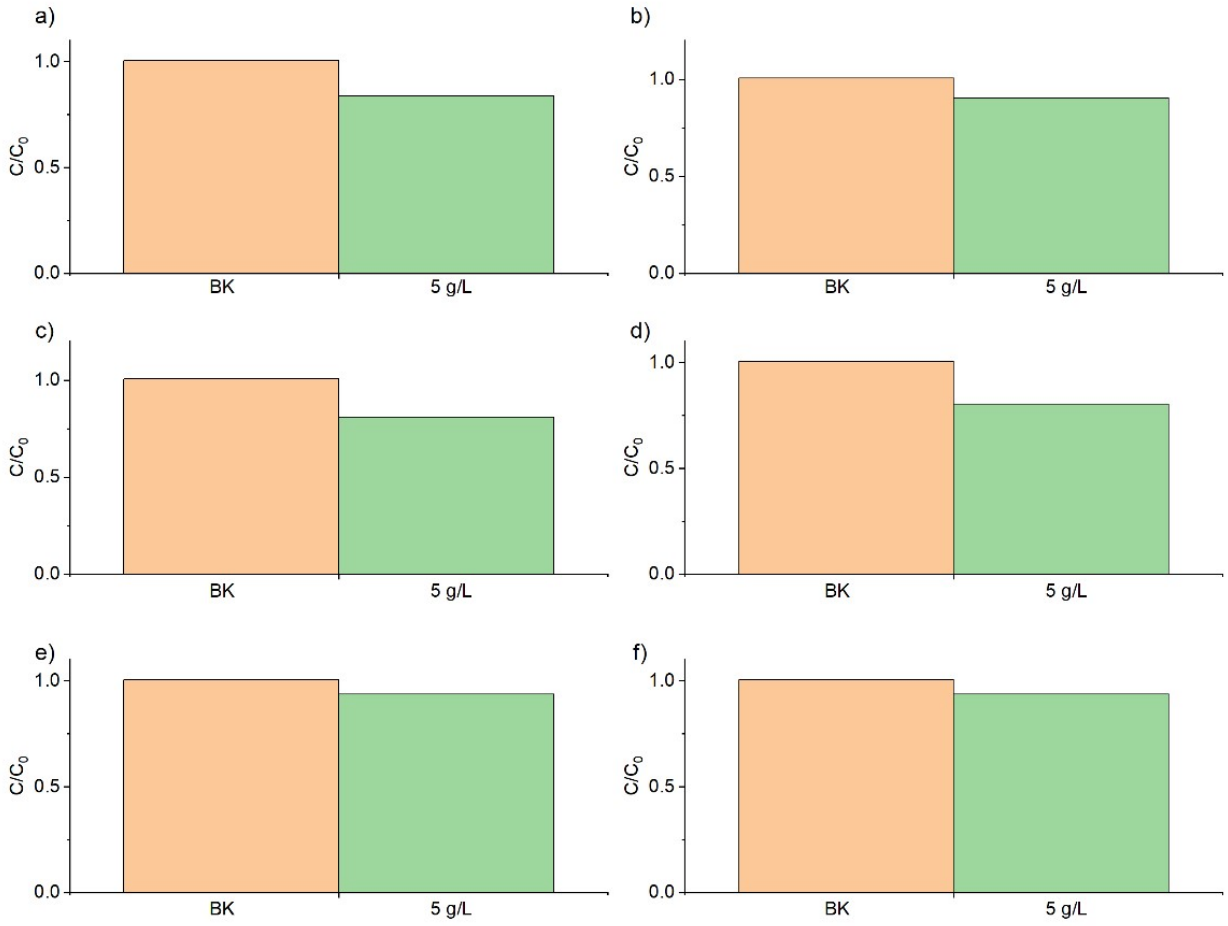

Figure S3 PFOA removal test using 5 g/L of pristine nZVI at a) pH 3 (PFOA 0.2 mg/L), b) pH 3 (PFOA 2 mg/L), c) pH 5 (PFOA 0.2 mg/L), d) pH 5 (PFOA 2 mg/L), e) pH 7 (PFOA 0.2 mg/L) and f) pH 7 (PFOA 2 mg/L) (Blank= BK without nZVI).

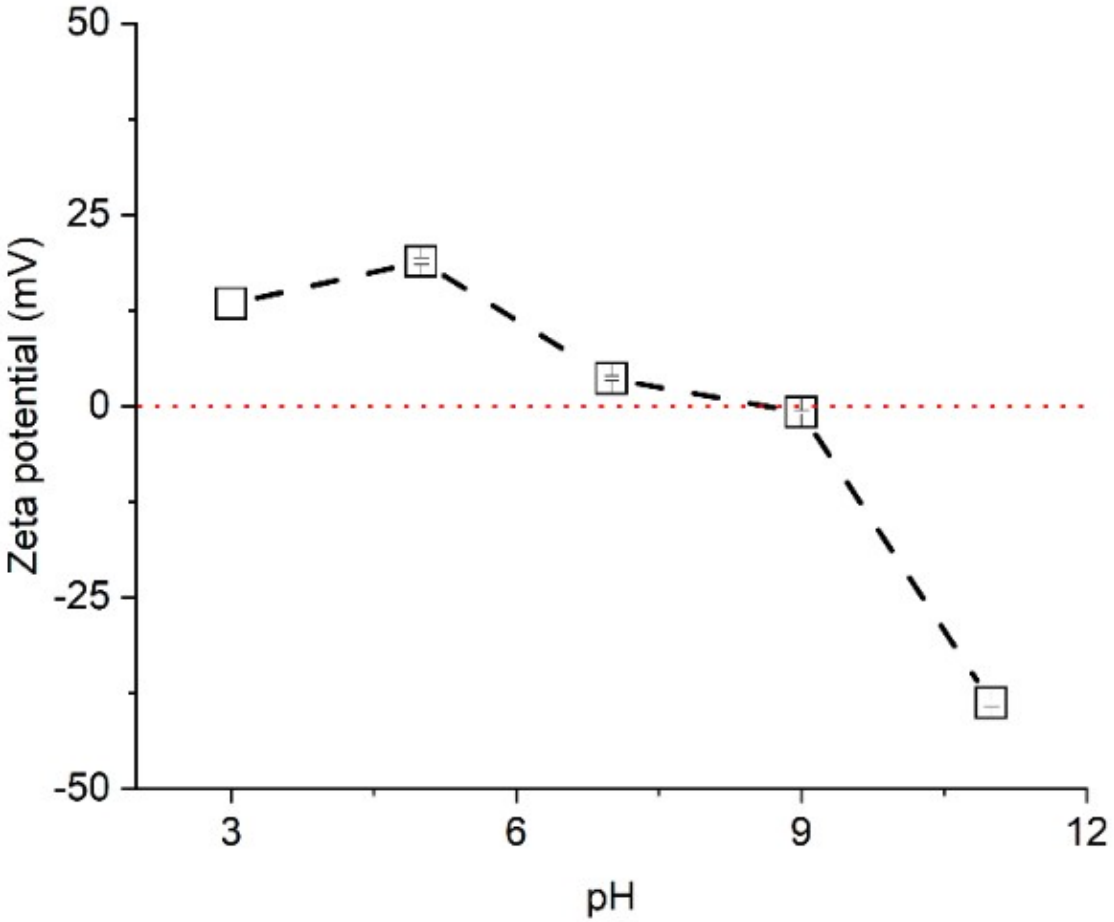

Figure S4 Zeta potential of nFe-CMBCD at various pH (material was synthesized using 2 g/L of carboxymethyl-β-cyclodextrin).

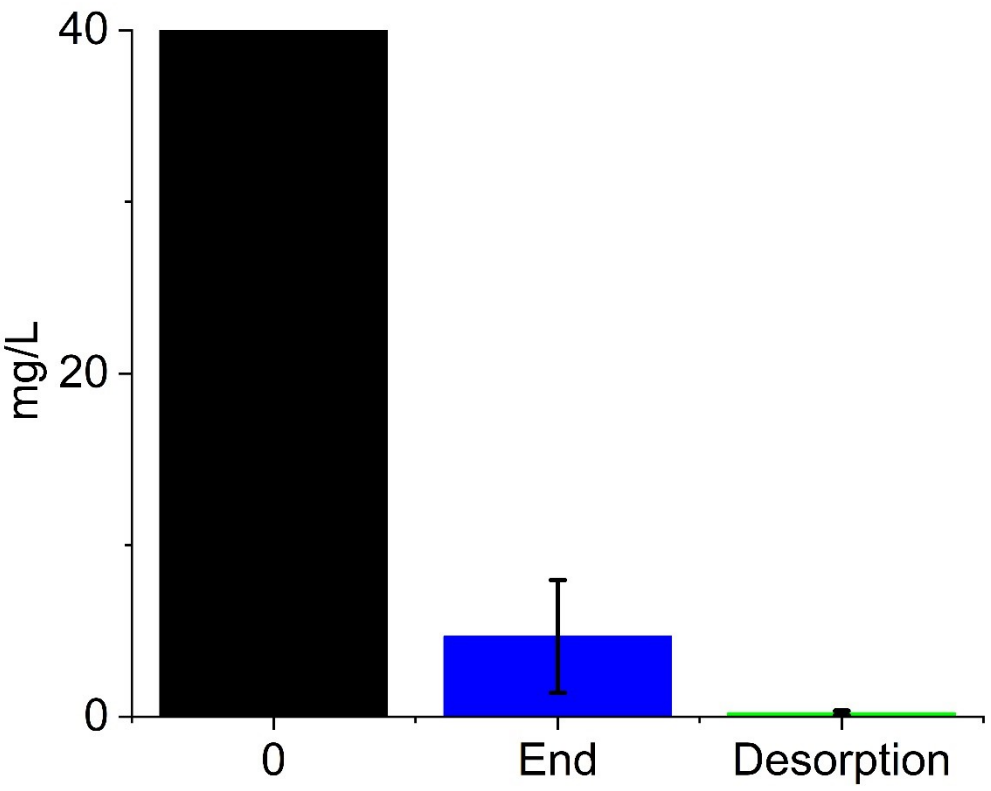

Figure S5 PFOA desorption test at the initial concentration of 40 mg/L (PFOA 40 mg/L, Fe-CMBCD 5 g/L, pH 7), the tests were carried out in duplicate.

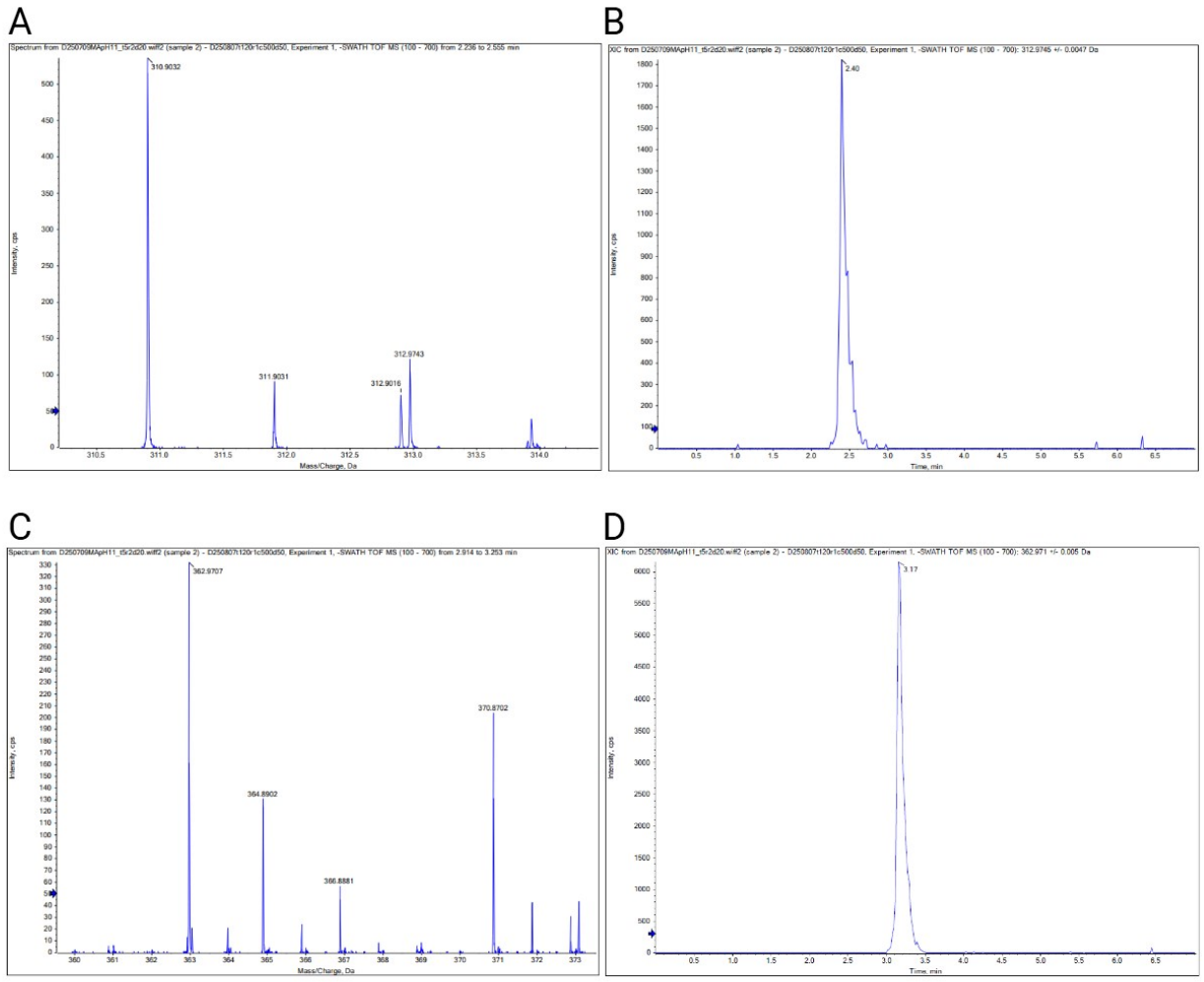

Figure S6 MS-MS detection of A-B) perfluoroheptanoic acid (312.9743 *m/z*) and C-D) perfluorohexanoic acid (362.9707).

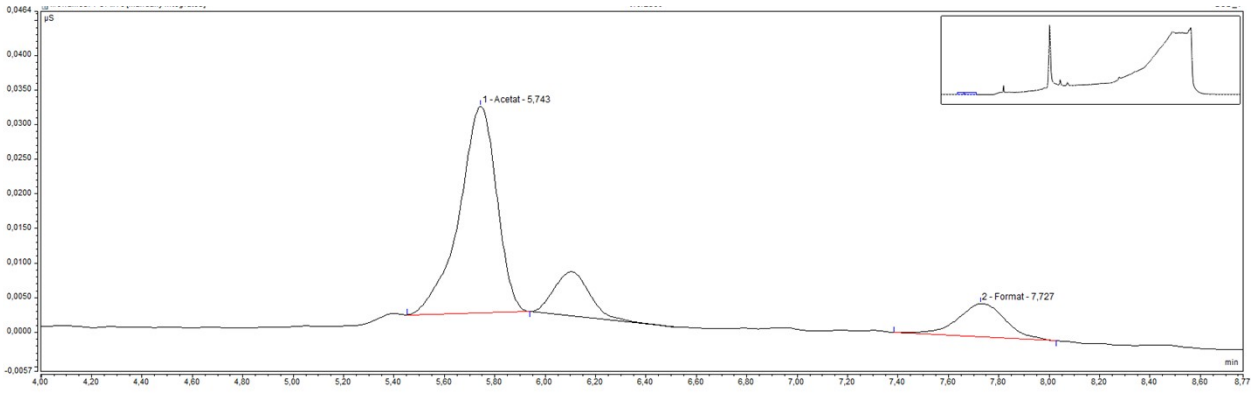

Figure S7 Acetate and formate detection.

Equations

$Fe^0+2H_2O \rightarrow Fe^{2+}+H_2+2OH^-$ (1)

$2Fe^0+O_2+2H_2O \rightarrow 2Fe^{2+}+4OH^-$ (2)

$6Fe^{2+}+O_2+6H_2O \rightarrow 2Fe_3O_4+12H^+$ (3)

$Fe^{2+}+2OH^- \rightarrow Fe(OH)_2$ (4)

$6Fe(OH)_2+O_2 \rightarrow 2Fe_3O_4+6H_2O$ (5)

$4Fe^0+3O_2+2H_2O \rightarrow 4\gamma\text{-}FeOOH$ (6)

$4Fe_3O_4+O_2+6H_2O \rightarrow 12\gamma\text{-}FeOOH$ (7)

$\gamma-Fe_2O_3+H_2O \rightarrow 2\gamma\text{-}FeOOH$ (8)

Tables

Tab. S1. The linear gradient profile of the method used

Time	%A
0	70
0,2	70
5	10
6	10
6,2	70
8	70

Tab. S2. The transitions used to detect the PFAS.

Compound	precursor	fragment	DP	CE
PFHxA 1	312.97	118.992	-15	-25
PFHxA 2	312.97	268.982	-15	-15

PFHpA 1	362.97	168.989	-25	-25
PFHpA 2	362.97	118.992	-25	-25
PFOA 1	412.97	168.989	-25	-29
PFOA 2	412.97	368.977	-25	-20
$^{13}C_8$PFOA	420.99	171.999	-25	-29
$^{13}C_8$PFOS	506.96	79.957	-65	-93

DP denotes declustering potential and CE denotes collision energy used for the transition.

Tab. S3 A comparison of the different PFOA degradation processes.

Process	**PFOA Conc.**	**Removal (%)**	**k_{app} (min^{-1})**	**pH**	**Time**	**Reference**
Persulfate-assisted electrochemical oxidation	50 µg/L	99.9	0.078	4.5	2 h	[8]
nZVI@NCF/PMS	1mg/L	84.4	0.013	7.0	2 h	[9]
nZVI/rGO	1 mg/L	98.2	-	4.2	24 h	[10]
ISBC/PMS	2 mg/L	99.9	0.054	6.4	2 h	[11]
UV/phenol/DTN	0.5 mg/L	-	0.002	3.5	3.5 h	[12]
Si-nZVI	1 mg/L	96	-	7.0	48 h	[13]
nFe-CMBCD	0.2 – 2 mg/L	99.2 - 99.8	~0.57–~0.74	3.0	10 min	This work

References

1 D. Silvestri, S. Wacławek, B. Sobel, R. Torres–Mendieta, M. Pawlyta, V. V. T. Padil, J. Filip and M. Černík, *Separation and Purification Technology*, 2021, **257**, 117880.

2 K. Krawczyk, S. Wacławek, D. Silvestri, V. V. T. Padil, M. Řezanka, M. Černík and M. Jaroniec, *Journal of Colloid and Interface Science*, 2020, **586**, 655–662.

3 A. Liu and W. X. Zhang, *Analyst*, 2014, **139**, 4512–4518.

4 X. Yang, S. Yu, M. Wang, Q. Liu, X. Jing and X. Cai, *Chemical Engineering Journal*, 2022, **431**, 133370.

5 K. Krawczyk, D. Silvestri, N. H. A. Nguyen, A. Ševců, D. Łukowiec, V. V. T. Padil, M. Řezanka, M. Černík, D. D. Dionysiou and S. Wacławek, *Science of The Total Environment*, 2022, **817**, 152888.

6 A. Z. M. Badruddoza, A. S. H. Tay, P. Y. Tan, K. Hidajat and M. S. Uddin, *Journal of Hazardous Materials*, 2011, **185**, 1177–1186.

7 S. Zhu, S. H. Ho, X. Huang, D. Wang, F. Yang, L. Wang, C. Wang, X. Cao and F. Ma, *ACS Sustainable Chemistry and Engineering*, 2017, **5**, 9673–9682.

8 S. Annamalai, N. Kim and S. Hwang, *Journal of Environmental Chemical Engineering*, 2025, **13**, 119424.

9 C. Li, C. Shen, B. Gao, W. Liang, Y. Zhu, W. Shi, S. Ai, H. Xu, J. Wu and Y. Sun, *Chemosphere*, 2024, **351**, 141209.

10 S. Regmi, M. S. Sarker, A. K. Oglesby, K. N. Banning, E. E. Lanier, C. Xia, S. T. Sabuj, H. Yang, N. Khan and J. Liu, *Journal of Hazardous Materials*, 2025, **497**, 139586.

11 S. Fu, Y. Zhang, X. Xu, X. Dai and L. Zhu, *Chemical Engineering Journal*, 2022, **450**, 137953.

12 X. Xiong, Z. Luo, S. Luo, L. Bai, Y. Shang, A. L. Junker and Z. Wei, *Water Research*, 2025, **279**, 123401.

13 M. Liao, S. Zhao, G. Zhan, J. Liang, Z. Li, F. Dong, Y. Pan, H. Li and L. Zhang, *J. Am. Chem. Soc.*, 2025, **147**, 3402–3411.